The Effect of a Porous Medium on the Flow of a Liquid Vortex

Fatemeh Hassanipour   fatemeh@utdallas.edu
Department of Mechanical Engineering
University of Texas at Dallas
Richardson, TX 75080, USA

Jose L. Lage
Department of Mechanical Engineering   jll@lyle.smu.edu
Southern Methodist University
Dallas, TX 75205, USA

Abstract

This study investigates the predominant criteria in the persistence or decay of vortex flows in porous media. A simple approach is used to build a pair of vortices in a fluid. The vortices impinge on a permeable wall, thus allowing a study of the interaction of vortices with the porous medium. New insights are obtained, among them that permeability has a more important effect on this interaction compared with either porosity or the vortex transport velocity.

Keywords: vortex flow, porosity, permeability

1. INTRODUCTION

Modeling and simulation of vortical flow through permeable (porous) media are essential for the design of new devices and the prediction of a myriad of natural and man-made processes, such as metal (alloy) processing, beach erosion, forest fires, snow avalanche, grain storage, underground flow, and alveolar respiration. In forestry, accurate simulation of turbulent air flow through the vegetative porous medium can predict the spread of forest fires as well as the spreading of seeds that result in biodiversity. Dispersion of smog in heavily built cities can be accurately modeled by turbulent flow in porous media. The aerial spreading of hazardous substances in a city is similarly modeled, with applications in homeland security. Detection of biological and biochemical compounds in permeable fabrics via turbulent air "puffs" is yet another application. In energy exploration, the flow of oil and gas along a radial-inward path in an oil well is accelerated by turbulence arising as the flow reaches a more permeable region (the well).

Our study involves vortex flows and porous media, two subject matters that can individually be complex and interesting on their own. The issue of vortex flow in porous media begins with transition from laminar flow behavior to turbulence flow. Transition to turbulence in porous media is among the interesting topics reviewed by Getachew et al [1] who discussed several experimental studies related to transition to turbulence in porous media, and by Inoue et al [2]. Vortex rings are also used by other investigators to unveil the basic structure of a turbulent round jet by Lau and Fisher [3] and the dynamics of coherent structures in turbulent boundary layers by

Fatemeh Hassanipour & Jose L. Lage

Lim [4]. Moreover, Chu and Falco [5] used laminar vortex rings interacting with an inclined, moving wall to reproduce some of the features observed in turbulent boundary layers. In addition to laminar vortex rings, other investigations have studied the entrainment, growth, and turbulence production in turbulent vortex rings to better understand the role of coherent structures in turbulence by Maxworthy [6], Glezer et al. [7] and Olcay et al.[8]. However, the behavior of vortex flow in porous media has not been directly studied.

The interaction of vortex flows and porous media is on the cutting edge of knowledge in fluid mechanics. Vortex flows are inherently nonlinear and are known to display intriguing behavior while interacting with boundary conditions and various flow conditions. Porous media also with their various morphologies are a challenging area of ongoing study. When these two subject areas come together, an even richer set of conditions emerge and, as shown by the analysis in the sequel, display interesting behaviors.

The current study investigates the transport of large vortical structures through permeable obstructions. The focus on large-scale vortical structures is motivated by their intricate local transport behavior depending on the characteristics of the permeable obstruction. This study aims at building a protocol for predicting the behavior of vortical flow based on permeable media and flow characteristics. Numerical simulations demonstrate the effect of permeable media properties and vortex strength on the transport of vortex flow in porous medium.

2. MODEL CONFIGURATION

A simplified two-dimensional model is used, shown in Figure 1. The vortex ring generator is a piston–cylinder mechanism located in a 160 x 60 x 60 cm water tank. The cylinder is 50 cm long with a diameter of 5cm, which is used to produce a finite-duration jet pulse. The jet velocity program is trapezoidal to create a vortex flow, Fig 2.

The vortex ring impinges to a 40 x 20 x 20 cm porous medium located within 40 cm in front of it. Porous media with various morphologies are characterized by the porosity$(\emptyset)$ and permeability(K).
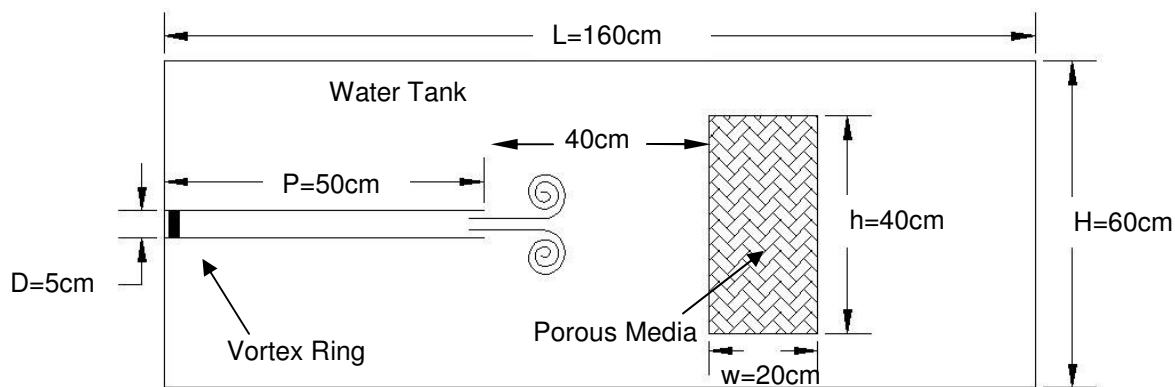

FIGURE 1: Schematic model configuration

The test is repeated with two different velocities of 0.179 $\frac{m}{s}$ and 0.058 $\frac{m}{s}$. Jet Reynolds number (Re) is calculated based on the piston's maximum velocity (U), piston diameter (D) and the fluid viscosity (ν), namely,

$$Re_j = \frac{UD}{\nu} \qquad (1)$$

Two velocity profiles by the vortex ring generator are:

Case 1: Re (jet)=9000

$$\begin{cases} u(t) = 0.324 * t & \text{if} & t < 0.554 \\ u(t) = 0.179 & \text{if} & 0.554 \leq t \leq 4.978 \\ u(t) = -0.323 * t + 1.79 & \text{if} & t > 4.978 \end{cases} \qquad (2)$$

Case 1: Re (jet)=3000

$$\begin{cases} u(t) = 0.104 * t & \text{if} & t < 0.554 \\ u(t) = 0.058 & \text{if} & 0.554 \leq t \leq 4.978 \\ u(t) = -0.104 * t + 0.577 & \text{if} & t > 4.978 \end{cases} \qquad (3)$$

These profiles are obtained based on the extracted data from experimental set up made.

Fatemeh Hassanipour & Jose L. Lage
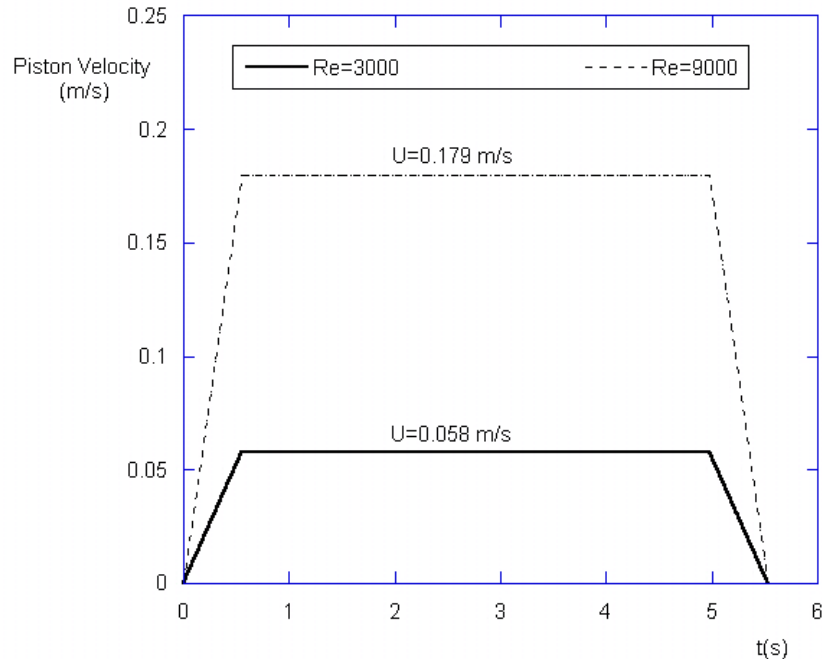
FIGURE 2: Typical Trapezoidal piston velocity for Re=3000 and Re=9000

3. THEORETICAL FORMULATION

The general equation for fluid flow through an isotropic, rigid, homogenous porous medium is Brinkman-Hazen-Dupuit-Darcy equation: [1]

$$0 = -\nabla(\emptyset \overline{p}) + \mu_e \nabla^2 u' - \left[\frac{\mu}{K}\emptyset u' + C\rho\emptyset^2 |u'|u'\right] \qquad (4)$$

Observe that Equation 4 has six physical properties: fluid density ρ, fluid dynamic viscosity μ, effective viscosity μ_e, permeability K, form coefficient C, and porosity $\emptyset$. The latter is defined as:

$$\emptyset = {A_f}\big/{A_t} \qquad (5)$$

A_f is the area occupied by the fluid and A_t is the total volume of the mateiral. Parameter ρ, μ, $\emptyset$ can be measure independently but the other three namely μ_e, K and C depends on the geometry of the permeable medium. They cannot be measured directly, nor calculated analytically, because there is no model relating them to more basic (measurable) quantities valid for all porous media. In principle, these quantities should be obtained simultaneously by matching the solution of Equation 4 to experimental data.

The Brinkman-Hazen-Dupuit-Darcy equation also has an alternative form where C is replaced by $\frac{C_f}{\sqrt{K}}$. The constant C_f is often takes the value 0.55.

$$c = \frac{C_f}{\sqrt{K}} \qquad (6)$$

In our study K varies from 10^{-8} to 10^{-2}. Porosity changes from 0.2 to 0.8, and the value for C varies accordingly, as listed in Table 1.

$K\ (m^2)$	$\varnothing$	$C\ (^1/_m)$
$10^{-8} \rightarrow 10^{-2}$	$0.2 \rightarrow 0.8$	$5.5 \rightarrow 5500$

TABLE 1: Tables Representative of porous media properties

4. SIMULATION

A structured grid technique is adopted for accelerating the convergence to the steady-state. As a reference criterion, average vorticity of the flow is calculated by numerical methods to achieve an optimum grid (ΔG) and time interval (Δi) size. Vorticity (ω) is found mathematically at a point for each element of fluid that is a vector and is defined as the curl of the velocity

$$\vec{\omega_i} = \vec{\nabla} \times \vec{V_i} = \left(\frac{\partial v_i}{\partial x} - \frac{\partial u_i}{\partial y} \right) \qquad (7)$$

The average vorticity, $\vec{\omega}_{avg}$ in a small region of fluid flow is defined as the circulation around the boundary of the small region, divided by the area A of that region.

$$\vec{\omega}_{avg} = \frac{\sum_{i=1}^{n} \vec{\omega_i}}{w \times h} \qquad (8)$$

Where w and h are the porous medium dimensions.

In Table 2, representative results for ω_{avg} show that the optimum grid size of 0.5 cm and interval time of 0.125 seconds are good values for running the simulation.

ΔG (cm)	Δi (s)	1/s
1.00	0.500	0.0086
0.50	0.500	0.0118
0.25	0.500	0.0104
1.00	0.250	0.0080
0.50	0.250	0.0096
0.25	0.250	0.0093
1.00	0.125	0.0078
0.50	0.125	0.0093
0.25	0.125	0.0092

TABLE 2: Representative grid and time interval accuracy for Re=9000

The mathematical formulation for the vortex flow behavior in porous media is solved by the finite volume method with successive over-relaxation. The Solver method is segregated and second-order accurate in space. The porous media object is modeled by the addition of a momentum source term to the standard fluid flow equations. The source term is composed of two parts: a viscous loss term (Darcy) and an inertial loss term:

$$0 = -\nabla(\emptyset \overline{p}) + \mu_e \nabla^2 u' + [S_i] \tag{8}$$

where
$$S_i = \left(\frac{\mu}{\alpha}v_i + C_2 \frac{1}{2}\rho[(v]_{mag}.v_i)\right) \tag{9}$$

α is the permeability, $\frac{1}{\alpha}$ is the viscous resistance coefficient (1/m2), and C_2 is the inertial resistance factor (1/m). If we compare Equations 4,8 and 9, then:

$$\frac{\mu}{K}\emptyset = \frac{\mu}{\alpha} \quad \rightarrow \quad \frac{1}{\alpha} = \emptyset\frac{1}{K} \tag{10}$$

and

$$C_2\frac{1}{2}\rho = C\rho\emptyset^2 \quad \rightarrow \quad C_2 = 2C\emptyset^2 \tag{11}$$

Table 3 shows the modified values based on the new parameters in Equation 8 for running the simulation to investigate the transport phenomena of vortex flow in porous media.

Re	$\emptyset$	$K\,(m^2)$	$C\,(^1/_m)$	$C_2\,(^1/_m)$	$\frac{1}{\alpha\left(\frac{1}{m}^2\right)}$
3000	0.2	10^{-2}	5.5	0.44	0.2×10^2
3000	0.2	10^{-8}	5500	440	0.2×10^8
3000	0.8	10^{-2}	5.5	7.04	0.8×10^2
3000	0.8	10^{-8}	5500	7040	0.8×10^8
9000	0.2	10^{-2}	5.5	0.44	0.2×10^2
9000	0.2	10^{-8}	5500	440	0.2×10^8
9000	0.8	10^{-2}	5.5	7.04	0.8×10^2
9000	0.8	10^{-8}	5500	7040	0.8×10^8

TABLE 3: Properties of various porous media and vortex strength used in simulation

5. RESULTS

Numerical analysis and simulations are performed to illustrate the transport of vortical flow with various velocities through porous media with various morphologies. The significance, expansion, contraction and separation of vortex flow is distinguishable in color-coded figures. Table 4 lists these figures and their relevant parameters.

Figure	Re	$K(m^2)$	$\emptyset$
3-a	3000	10^{-2}	0.2
3-b	3000	10^{-8}	0.2
3-c	3000	10^{-2}	0.8
3-d	3000	10^{-8}	0.8
3-e	9000	10^{-2}	0.2
3-f	9000	10^{-8}	0.2
3-g	9000	10^{-2}	0.8
3-h	9000	10^{-8}	0.8

TABLE 4: Vortex flow experiments and their parameters

In our numerical experiments, Reynolds number changes from 3000 to 9000 and porous media are used with different permeability and form-coefficient.

In Figure 3(a,c), vortex flow passes through the porous media for the minimum Reynolds number and maximum permeability. While propagating into the porous object, the lower vortex ring expands and partly blocks the upper vortex from traveling. Observation shows that the amount of porosity affects proportionally the size of vortex expansion.

For the same low Reynolds number but minimum permeability, the vortex pair does not pass through the porous object. The vortices mostly survive and return to the fluid with identical velocities. As observed in Fig. 3(b,d) separation of vortex rings does not occur. Investigation shows that in low permeability porous media and small Reynolds number flows, porosity has no effect on the behavior of vortex flow.

In another test, the Reynolds number was increased to 9000 and simulations repeated with the same porous permeability and porosities. When permeability is at maximum, the lower vortex ring expands, covers the whole porous medium and propagates through. Due to this quick expansion, it prevents the upper vortex from passing through the porous medium and makes it bounce back before making contact with the porous media. Returning to the flow, the upper vortex breaks into smaller vortexes in front of the porous object. Results show that the size and quantity of the split vortices are proportional to the porosity of the domain. See Fig. 3(e,g).

For the same Reynolds number of 9000 but minimum permeability, both vortex rings bounce back. In both porosities, a part of the lower vortex passes the porous medium and creates a new small vortex behind the porous medium (see Fig.3(f,h)). So, porosity does not affect the flow term when the Reynolds number is large and permeability of the porous medium is very low.

If compare the four figures, we observe that regardless of Reynolds number, vortex flows bounce back and cannot pass through a low-permeability porous medium. However, Reynolds numbers affect the expansion, breaking and return velocity of vortex rings. Permeability also plays an important role in the transport of vertical flow in the porous domain.

Figure 5 also shows the process of vortex flow movement in the porous media for case 1 and 8 for a duration of 312 seconds. Shots are taken in equal time intervals. Simulation reveals the areas in the domain that are more susceptible to the vortex streamlines.


(a) $\text{Re} = 3000, \varnothing = 0.2, K = 10^{-2}(\text{m}^2)$

(e) $\text{Re} = 9000, \varnothing = 0.2, K = 10^{-2}(\text{m}^2)$

(b) $\text{Re} = 3000, \varnothing = 0.2, K = 10^{-8}(\text{m}^2)$

(f) $\text{Re} = 9000, \varnothing = 0.2, K = 10^{-8}(\text{m}^2)$

(c) $\text{Re} = 3000, \varnothing = 0.8, K = 10^{-2}(\text{m}^2)$

(g) $\text{Re} = 9000, \varnothing = 0.8, K = 10^{-2}(\text{m}^2)$

(d) $\text{Re} = 3000, \varnothing = 0.8, K = 10^{-8}(\text{m}^2)$
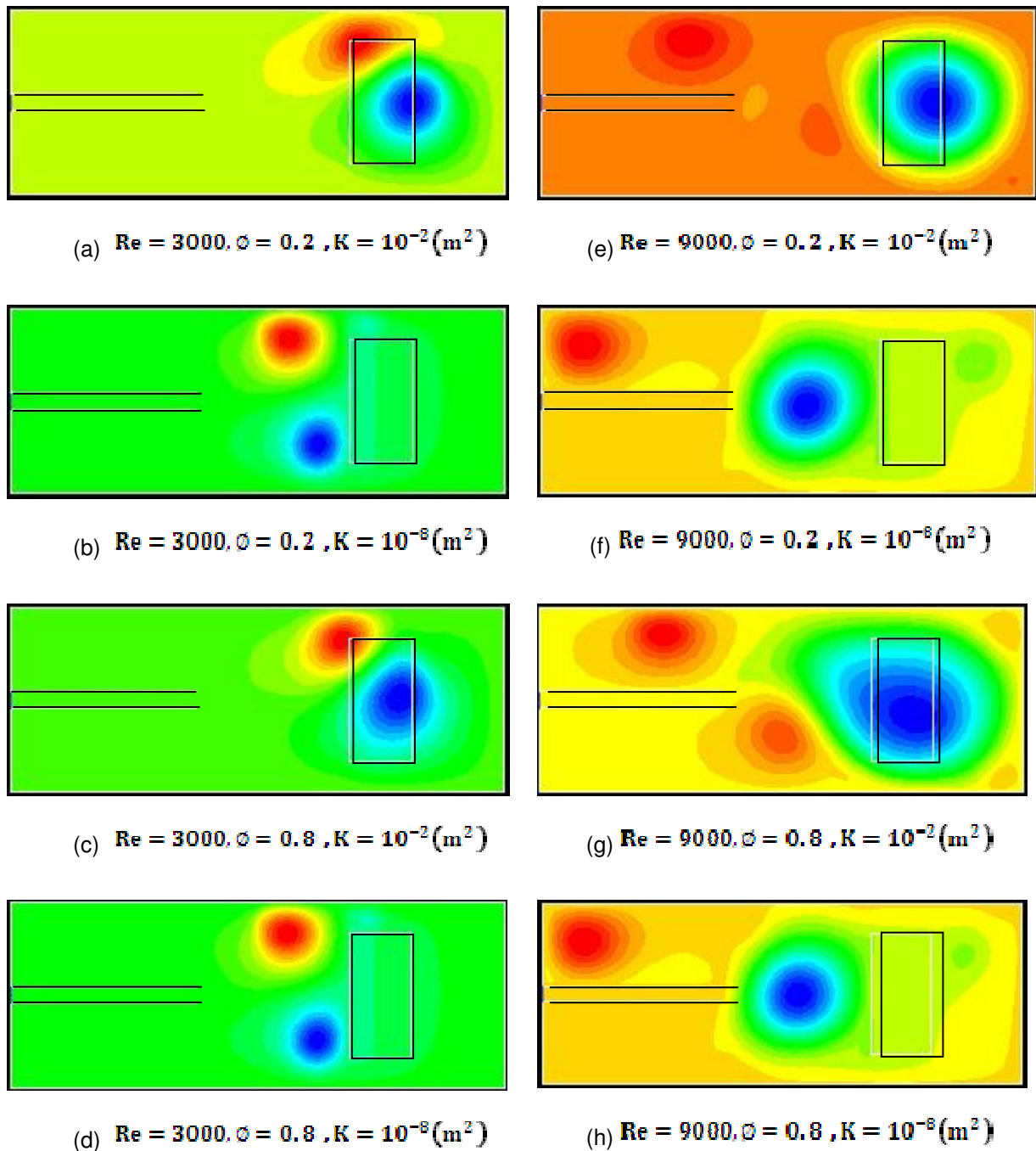
(h) $\text{Re} = 9000, \varnothing = 0.8, K = 10^{-8}(\text{m}^2)$

FIGURE 3: Local transport behavior of vertical flow in porous domain
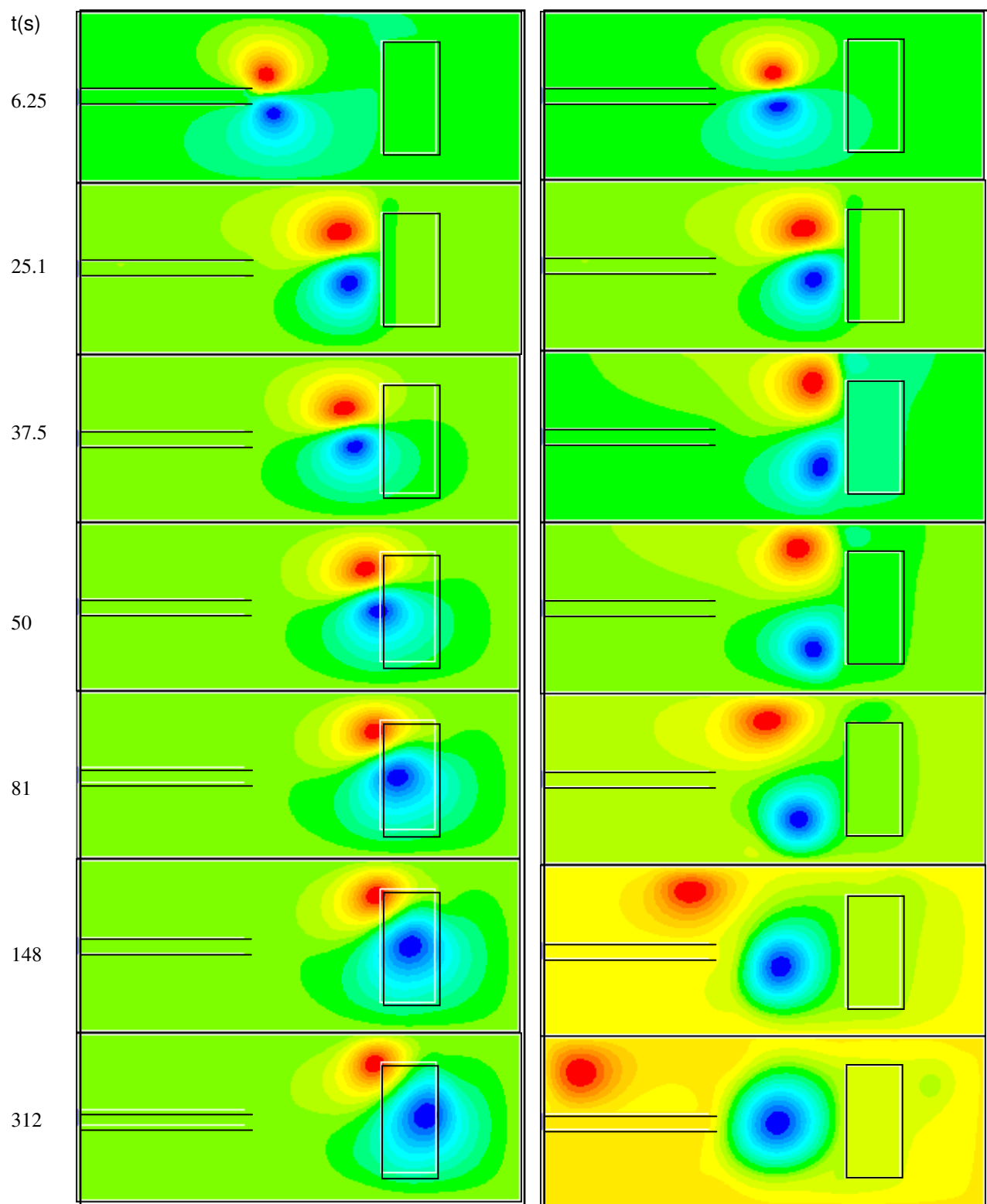
FIGURE 4: Process of vortex movement: Re=3000, $\emptyset = 0.2,$ $K = 10^{-2}\left(m^2\right)$ (left),
Re=9000, $\emptyset = 0.8, K = 10^{-8}\left(m^2\right)$ (right)

6. REFERENCES

1. D. Getachew, W.J. Minkowycz, J.L. Lage, "A modified form of the κ–ε model for turbulent flows of an incompressible fluid in porous media". International Journal of Heat and Mass Transfer, 43(16):2909-2915, 2000.

2. T Inoue, T Masuoka, Y Takatu, Flow Transition to Turbulence in Porous Media, National Heat Transfer Symposium of JAPAN 2000 - Japan Heat Transfer Society; 1999.

3. J.C. Lau, M.J. Fisher, "The vortex-street structure of turbulent jets", Part 1, Journal of Fluid Mechanics Digital Archive: 299-337, 2006.

4. T.T. Lim, "On the breakdown of vortex rings from inclined nozzles", Physics of Fluids, 1998.

5. C.C. Chu, R.E. Falco, "Vortex ring/viscous wall layer interaction model of the turbulence production process near walls". Journal of Experiments in Fluids, 305-315, 1987.

6. T. Maxworthy, Journal of Fluid Mechanics Digital Archive, 465-495, 1977.

7. A. Glezer, D. Coles, "Journal of Fluid Mechanics Digital Archive, An experimental study of a turbulent vortex ring": 243-283, 1990

8. A.B. Olcay, P. Krueger, "Measurement of ambient fluid entrainment during laminar vortex ring formation". Journal of Experiments in Fluids: 235-247, 2007